ISSN: 2993-6594

Research Article

Open Access Journal of Disease and Global Health

Expression Status and Potential Therapeutic Value of M6A in Autism Spectrum Disorder

Li Yao, Yihuan Yue and Jinhui Wang*

Xiamen Hospital (Xiamen Children's Hospital), Children's Hospital of Fudan University, China

***Corresponding Author**
Jinhui Wang, Xiamen Hospital (Xiamen Children's Hospital), Children's Hospital of Fudan University, China.

Submitted: 2025, June 02; **Accepted:** 2025, July 01; **Published:** 2025, July 18

Citation: Yao, L., Yue, Y., Wang, J. (2025). Expression Status and Potential Therapeutic Value of M6A in Autism Spectrum Disorder. *Ope Acce Jou Dis Glo Heal, 3*(2), 01-15.

Abstract

Autism Spectrum Disorder (ASD), a neurodevelopmental disorder, is characterized by social deficits, repetitive behaviors, and restricted interest. In this study, the objective was to examine variations in m6A-modified gene expression among patients with ASD and to assess their correlation with immune cell infiltration. Gene expression data obtained from the Gene Expression Omnibus (GEO) database were processed using the Limma package to identify differentially expressed genes. Molecular m6A methylation regulator subtypes were constructed using ConsensusClusterPlus, and hub m6A regulators were identified using Least Absolute Shrinkage and Selection Operator (LASSO) regression and Support Vector Machine-Recursive Feature Elimination (SVM-RFE). Protein-protein interaction networks were established using starBase2.0 and depicted using Cytoscape.In total, 6,277 differentially expressed genes were identified. Notably, m6A regulators displayed significant differential expression in samples from patients with ASD. LASSO and SVM-RFE analyses underscored WTAP and RBM15 as key autistic-associated elements. These results indicate that WTAP and RBM15 modifications significantly contribute to ASD pathogenesis by influencing gene expression profiles and variations in the immune microenvironment. Deciphering the mechanism of action of ASD has revealed actionable strategies for precise therapy development.

Keywords: Autism Spectrum Disorder, N6-methyladenosine, WTAP, RBM15, Neurodevelopmental Disorders.

1. Introduction

As a clinically diverse neurodevelopmental entity, ASD manifests as impaired socioemotional reciprocity and rigid behavioral and interest patterns. The incidence of ASD has been progressively increasing, with current estimates indicating that it affects approximately 2.27% of US children [1]. Despite the growing awareness and understanding of ASD, its underlying mechanisms of action and effective therapeutic interventions remain elusive. Current diagnostic and therapeutic approaches primarily focus on behavioral assessments and interventions that often fail to address the biological underpinnings of the disorder [2].

One notable challenge in ASD research is the heterogeneity of the disorder. ASD presents with a diverse array of symptoms and associated comorbidities, such as immune dysregulation and gastrointestinal complications [3]. Furthermore, m6A modification disruption is associated with numerous neurodevelopmental and neuropsychiatric disorders, making it a promising area of investigation in ASD therapy [4]. Emerging evidence suggests that m6A modifications influence immune responses and neuroinflammation, which are critical components in the etiology of ASD [5]. m6A regulators are differentially expressed in individuals with ASD, and these alterations may contribute to aberrant immune cell infiltration and activation in the brain [6]. The epigenetic interplay between m6A modifications and immune dysregulation in patients with ASD highlights the need for a thorough examination of m6A-modified genes and their influence on immune cell infiltration in such patients.

This study primarily focused on identifying differential m6A epitranscriptomic signatures in persons diagnosed with ASD, investigate their association with immune cell infiltration,

construct and validate molecular subtypes associated with immune infiltration, elucidate the molecular mechanisms underlying ASD, and identify prospective diagnostic biomarkers and therapeutic targets.

2. Results

2.1. Experimental Design

In this study, we compared the expression profiles of m6A regulatory components between ASD and control samples using the expression dataset derived from the GEO repository, data on the individual GEO microarrays used in our analysis are listed in Table 1. Subsequently, LASSO and SVM regression were used to identify potential diagnostic biomarkers, with functional and immune microenvironment deconvolution. Molecular subtypes and immune correlation analyses were conducted based on the m6A regulatory factors and immune cells, respectively (Figure 1).

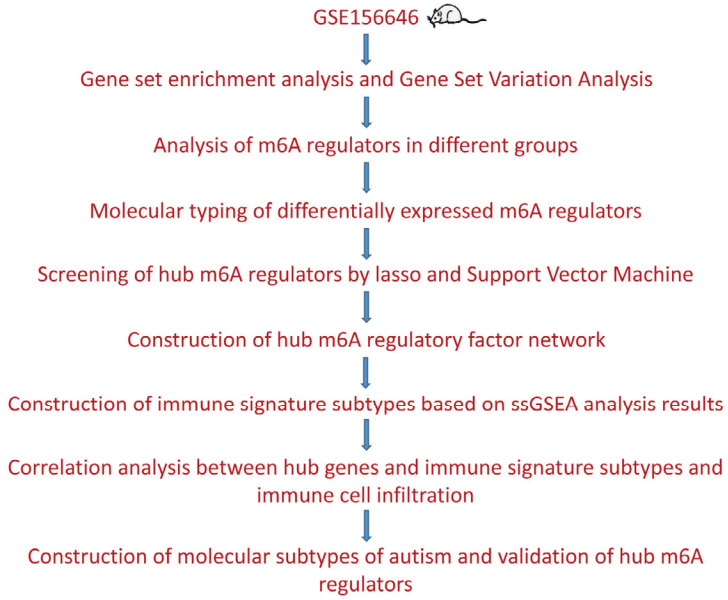

Figure 1: Flowchart

Data	normal	Autistic disorder
GSE156646	4 (50%)	4 (50)

Table 1: GSE156646-derived Biological Specimens.

2.2. Differential Gene Expressions between ASD and Control Tissues

To evaluate the impact of gene expression in spinal nerve ligation and normal tissues, Gene expression disparities were identified through the Limma framework (v3.50.0) on the integrated gene expression matrix. This analysis revealed 6,277 differentially expressed genes (DEGs) between ASD and control samples, comprising 5,683 upregulated and 594 downregulated genes (Figure 2a). The principal component analysis (PCA) results showed that ASD had a higher separation quality than the normal group (Figure 2b), and the peak expression results indicated that the expression matrix data quality was high (Figure 2c).

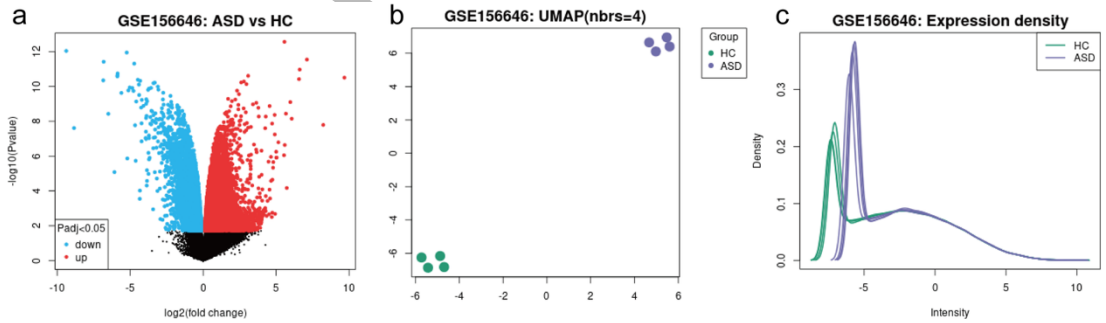

Figure 2: Differential expression analysis: a. Volcanic map of differential gene expression in ASD, b. PCA analysis of ASD and normal group, c. Peak gene expression analysis.

2.3. Gene Set Enrichment Analysis (GSEA)

To discern the functional disparities between ASD and normal tissues, we performed GSEA and GSVA on the two sample groups (Figure 3, Tables 2-3). GSEA enrichment profiling demonstrated a significant overrepresentation of Gene ontology (GO) biological processes within the ASD brain tissues, including aerobic respiration, amide biosynthetic processes, amine metabolic pathways, catabolic processes reliant on the anaphase-promoting complex,and antigen processing and presentation. The main enriched Kyoto Encyclopedia of Genes and Genomes (KEGG) results included Alzheimer's disease, oxidative phosphorylation, Huntington's disease, Parkinson's disease, and ribosomes (Figure 3a–b). The GSVA enrichment results showed that compared with normal tissues, ASD tissues had 49 and 53 significantly up- and downregulated GO functions, respectively, as well as 16 and 3 significantly up- and downregulated KEGG functions, respectively (Figure 3c, 3e), among which the significantly upregulated GO included Histamine secretion, Histone transport, UV protection, Platelet alpha granule membrane, and oxidized DNA binding. Significantly up-and downregulated GO terms encompassed cell proliferation regulation during kidney development, transmembrane receptor protein tyrosine kinase adapter activity, glucocorticoid receptor binding, and vinculin binding (Figure 3d). Significantly upregulated KEGG functions included tryptophan metabolism, other glycan degradation, propanoate metabolism, aminoacyl trna biosynthesis, selenoamino acid metabolism, and glycosphingolipid biosynthesis globo series; whereas significantly downregulated KEGG functions included mammal circadian rhythm and riboflavin metabolism (Figure 3f).

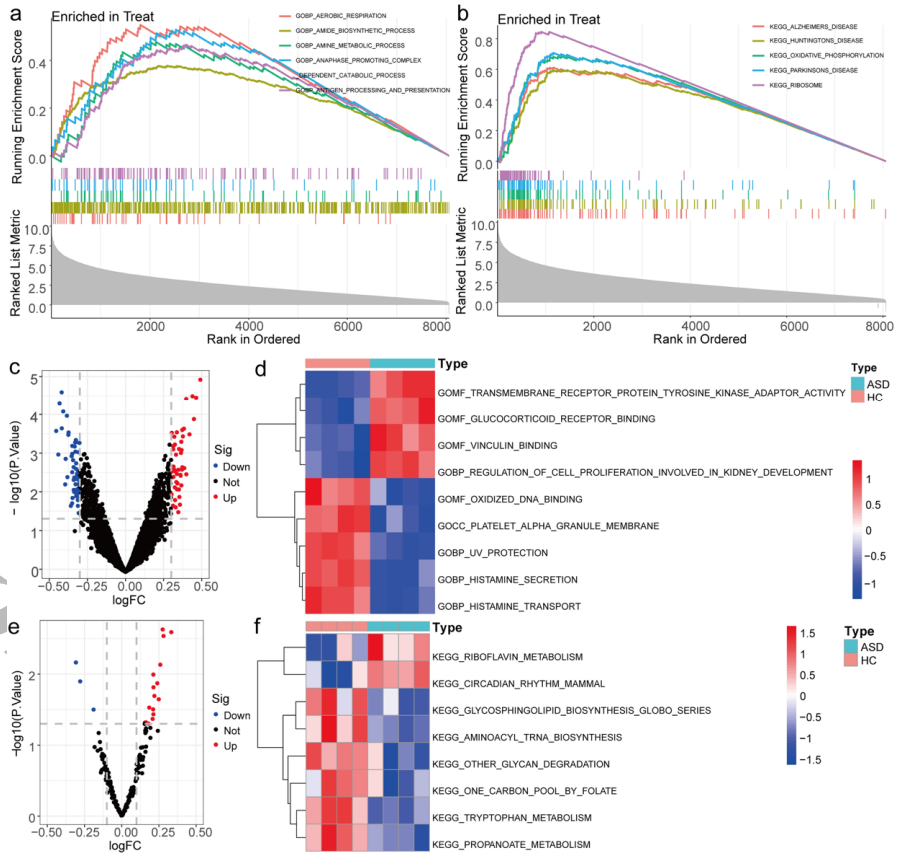

Figure 3: GSEA and GSVA enrichment analysis: a. GSEA-GO analysis, b. GSEA-KEGG pathway analysis, c. GSVA-GO volcano map analysis, d. GSVA-GO heatmap analysis, e. GSVA-GO volcano map analysis, f. GSVA-KEGG heat map analysis.

Description	Enrichment Score	NES	p.adjust
GOBP_AEROBIC_RESPIRATION	0.55	1.87	2.35E-02
GOBP_AMIDE_BIOSYNTHETIC_PROCESS	0.38	1.47	2.35E-02
GOBP_AMINE_METABOLIC_PROCESS	0.48	1.68	2.35E-02
GOBP_ANAPHASE_PROMOTING_COMPLEX_ DEPENDENT_CATABOLIC_PROCESS	0.53	1.82	2.35E-02
GOBP_ANTIGEN_PROCESSING_AND_ PRESENTATION	0.47	1.71	2.35E-02

GOBP_ANTIGEN_PROCESSING_AND_PRESENTATION_OF_PEPTIDE_ANTIGEN	0.49	1.76	2.35E-02
GOBP_APOPTOTIC_MITOCHONDRIAL_CHANGES	0.50	1.74	2.35E-02
GOBP_ATP_METABOLIC_PROCESS	0.53	1.98	2.35E-02
GOBP_ATP_SYNTHESIS_COUPLED_ELECTRON_TRANSPORT	0.70	2.48	2.35E-02
GOBP_AXO_DENDRITIC_TRANSPORT	0.50	1.74	2.35E-02
GOBP_CATION_TRANSPORT	0.35	1.36	2.35E-02
GOBP_CELL_ACTIVATION	0.32	1.26	2.35E-02
GOBP_CELL_ACTIVATION_INVOLVED_IN_IMMUNE_RESPONSE	0.37	1.40	2.35E-02
GOBP_CELL_MORPHOGENESIS_INVOLVED_IN_NEURON_DIFFERENTIATION	0.36	1.39	2.35E-02
GOBP_CELL_PART_MORPHOGENESIS	0.35	1.35	2.35E-02
GOBP_CELLULAR_COMPONENT_MORPHOGENESIS	0.33	1.30	2.35E-02
GOBP_CELLULAR_ION_HOMEOSTASIS	0.37	1.42	2.35E-02
GOBP_CELLULAR_KETONE_METABOLIC_PROCESS	0.44	1.60	2.35E-02
GOBP_CELLULAR_RESPIRATION	0.57	2.08	2.35E-02
KEGG_ALZHEIMERS_DISEASE	0.61	2.22	2.84E-09
KEGG_HUNTINGTONS_DISEASE	0.59	2.17	2.84E-09
KEGG_OXIDATIVE_PHOSPHORYLATION	0.69	2.43	2.84E-09
KEGG_PARKINSONS_DISEASE	0.71	2.51	2.84E-09
KEGG_RIBOSOME	0.84	2.99	2.84E-09
KEGG_OOCYTE_MEIOSIS	0.55	1.88	7.69E-05
KEGG_VIBRIO_CHOLERAE_INFECTION	0.61	1.97	2.08E-04
KEGG_GLYCOLYSIS_GLUCONEOGENESIS	0.61	1.96	3.35E-04
KEGG_CARDIAC_MUSCLE_CONTRACTION	0.53	1.80	3.65E-04
KEGG_VASOPRESSIN_REGULATED_WATER_REABSORPTION	0.61	1.93	3.65E-04
KEGG_PATHOGENIC_ESCHERICHIA_COLI_INFECTION	0.57	1.88	4.41E-04
KEGG_PROTEASOME	0.57	1.86	5.50E-04
KEGG_CALCIUM_SIGNALING_PATHWAY	0.46	1.65	5.92E-04
KEGG_GAP_JUNCTION	0.50	1.70	2.70E-03
KEGG_LONG_TERM_POTENTIATION	0.49	1.66	4.03E-03
KEGG_OLFACTORY_TRANSDUCTION	0.73	1.89	4.76E-03
KEGG_MELANOGENESIS	0.49	1.63	5.09E-03
KEGG_PENTOSE_PHOSPHATE_PATHWAY	0.66	1.82	9.78E-03

Table 2: Enriched Biological Pathways in GSE5546 Identified by GSEA.

id	logFC	P.Value
GOBP_HISTAMINE_SECRETION	0.49	1.20E-05
GOBP_HISTAMINE_TRANSPORT	0.44	3.23E-05
GOBP_UV_PROTECTION	0.40	3.79E-05
GOBP_REGULATION_OF_CELL_PROLIFERATION_INVOLVED_IN_KIDNEY_DEVELOPMENT	-0.38	1.08E-04

GOCC_PLATELET_ALPHA_GRANULE_MEMBRANE	0.46	3.54E-05
GOMF_TRANSMEMBRANE_RECEPTOR_PROTEIN_TYROSINE_KINASE_ADAPTOR_ACTIVITY	-0.42	2.55E-05
GOMF_GLUCOCORTICOID_RECEPTOR_BINDING	-0.43	5.20E-05
GOMF_VINCULIN_BINDING	-0.41	8.37E-05
GOMF_OXIDIZED_DNA_BINDING	0.45	1.32E-04
KEGG_TRYPTOPHAN_METABOLISM	0.28	2.36E-03
KEGG_OTHER_GLYCAN_DEGRADATION	0.33	2.57E-03
KEGG_PROPANOATE_METABOLISM	0.28	2.91E-03
KEGG_CIRCADIAN_RHYTHM_MAMMAL	-0.31	6.86E-03
KEGG_AMINOACYL_TRNA_BIOSYNTHESIS	0.26	7.38E-03
KEGG_SELENOAMINO_ACID_METABOLISM	0.21	1.02E-02
KEGG_RIBOFLAVIN_METABOLISM	-0.28	1.27E-02
KEGG_GLYCOSPHINGOLIPID_BIOSYNTHESIS_GLOBO_SERIES	0.24	1.35E-02

Table 3: Gene Set Variation Analysis of the GSE5546 Transcriptomic Landscape.

2.4. Expression Characteristics analysis of m6A Regulators in ASD

To investigate the epigenetic regulatory impact of m6A-associated machinery on ASD pathogenesis, we assessed the expression levels of 23 m6A regulators using Perl scripting and found that 15 m6A regulators (*HNRNPC, YTHDC1, YTHDF1, HNRNPA2B1, ZC3H13, YTHDF2, METTL16, WTAP, METTL3, RBM15B, YTHDF3, ALKBH5, FTO, CBLL1,* and *RBM15*) were included in this dataset.

Differential analysis showed seven differences in the expression of m6A regulators (*RBM15, ZC3H13, METTL3, HNRNPC, RBM15B, ALKBH5,* and *WTAP*) in the GEO dataset ($P < 0.05$, Figure 4a–b), which included one eraser and five writers (Figure 5). To assess the impact of m6A regulators on ASD tissues, co-expression analysis was conducted between m6A regulators in ASD/normal brain tissues (Fig 4c). RBM15B robust positive correlation (r = 0.91) was identified between the expression levels of RBM15B and ALKBH5, in contrast to the significant inverse relationship (r = -0.87) found in WTAP. Chromosomal analysis revealed the genomic locations of these genes (Figure 4d).

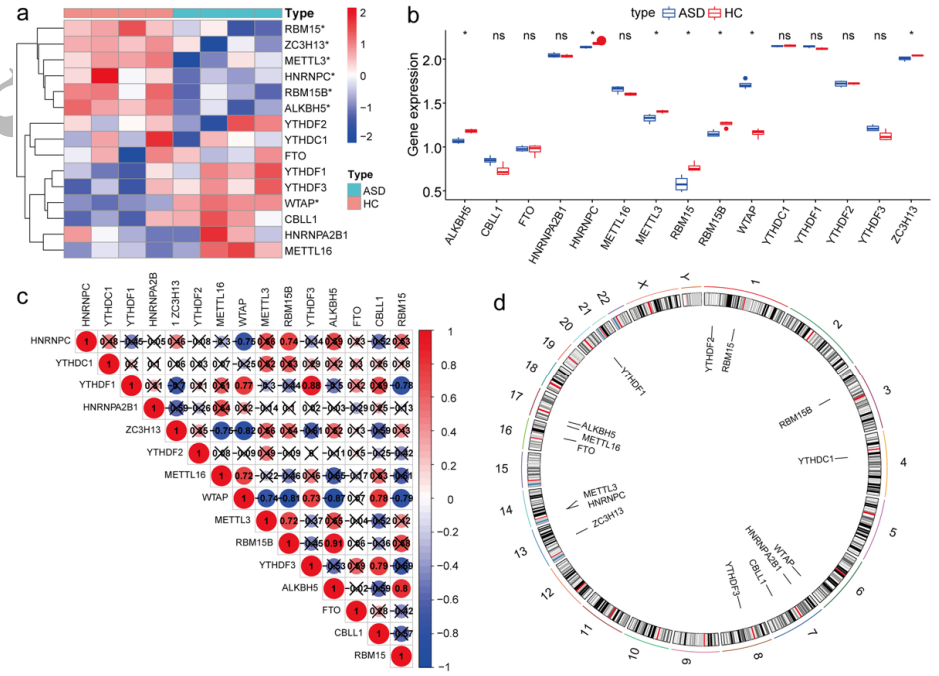

Figure 4: Expression profile of m6A regulators in ASD: a. M6A regulatory factor differential heatmap, b. m6A regulatory factor differential expression boxplot, c. m6A regulatory factor correlation analysis, d. m6A regulatory factor chromosome localization.

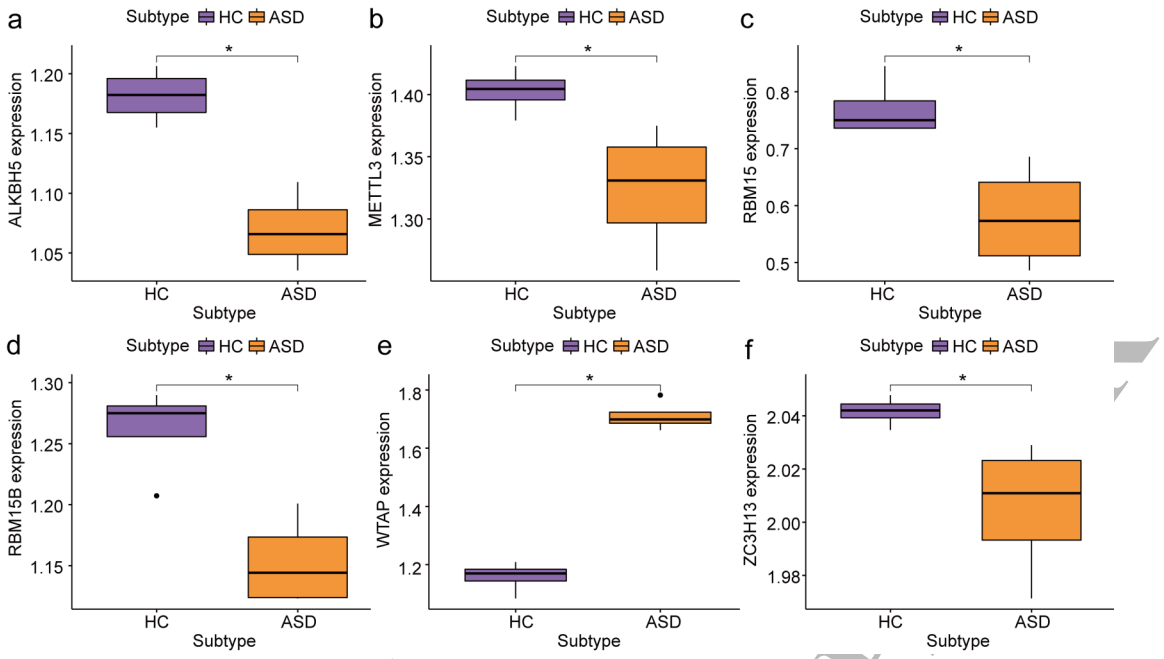

Figure 5: Writers and erasers differential expression analysis in ASD: a-f. differential m6A gene expression boxplot.

2.5. Molecular typing and related Analysis of M6A Regulators

To delineate the functional dynamics of m6A epigenetic modulators operating within the methylation-driven transcriptional landscapes of ASD specimens, we used the expression profiles of differentially expressed m6A regulators to perform hierarchical clustering across all samples in the GEO dataset. Clustering revealed two distinct isoforms (1: n = 4; 2: n = 4, as shown in Figures 6a–c), whereas PCA indicated a high resolution quality (Figure 6d).

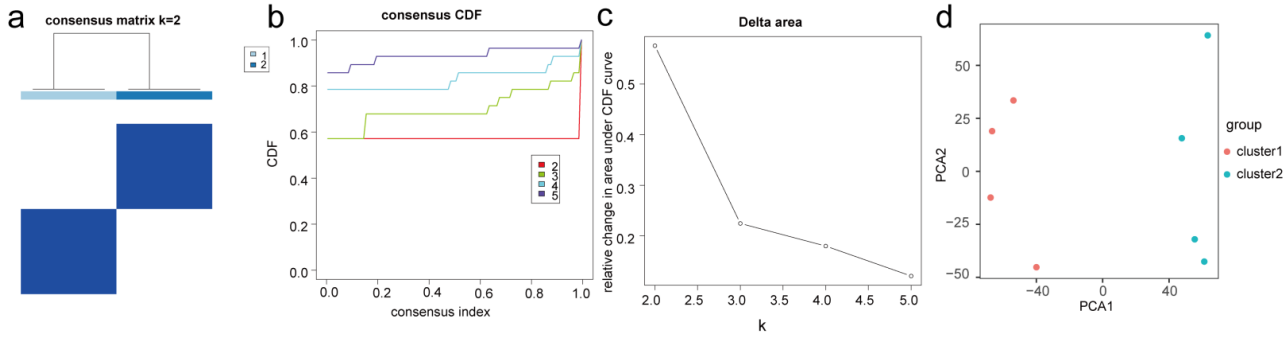

Figure 6: M6A regulators molecular isoform construction: a-c: Cluster grouping of samples based on differential expression of m6A regulatory factors, a: Sample size after grouping; b: The area under CDF and its relative variation with increasing k; c: The Delta area plot displays the relative change in area under the CDF curve; d: PCA analysis under Cluster 1 and Cluster 2 grouping, where red represents Cluster 1 and blue represents Cluster 2.

2.6. Constructing Prognostic models related to m6A Regulators and Screening key m6A Regulators

A five-gene prognostic signature comprising m6A regulatory components (WTAP, METTL3, RBM15B, ALKBH5, RBM15) was developed via LASSO regression (Figure 7a–b). To further screen hub m6A regulators in ASD, we employed the machine learning technique known as support vector machine recursive feature elimination (SVM-RFE) to examine m6A regulators in the normal and ASD groups and screened two characteristic genes (Figure 7c). We identified an intersection of five m6A regulators from the LASSO model and two m6A regulators derived from random forest tree analysis (Figure 7d) to obtain two key genes, WTAP and RBM15B.

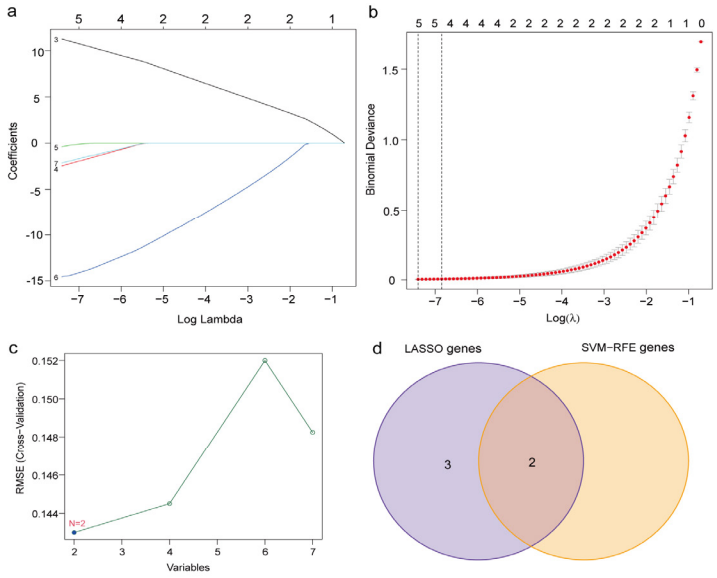

Figure 7: Screening of key m6A regulator: a-b: The regression coefficient in LASSO regression algorithm and the cross validation of adjusting parameter selection in proportional risk model will finally determine the best penalty value and screen the genes most related to autism; c: SVM ; d: Venn diagram is used to draw the intersection of LASSO and SVM to screen genes.

2.7. Gene and Function Analysis related to Hub Modifiers

We established a protein-protein interaction (PPI) network encompassing hub m6A regulators, where gene WTAP displayed the highest degree of interaction with 72 proteins, followed by gene RBM15B, which interacted with 25 proteins. Figure 7b–d shows that the two hub m6A regulators were regulated by multiple miRNAs, with WTAP having the most interacting miRNAs (737), followed by RBM15B (368 in total). To further examine the connections between the hub m6A regulators and transcription factors (TFs), we used a transcriptome expression matrix and Pearson correlation analysis to obtain the hub m6A regulators and two TFs from 1665 TFs. The hub m6A regulators were simultaneously regulated by EGR2.

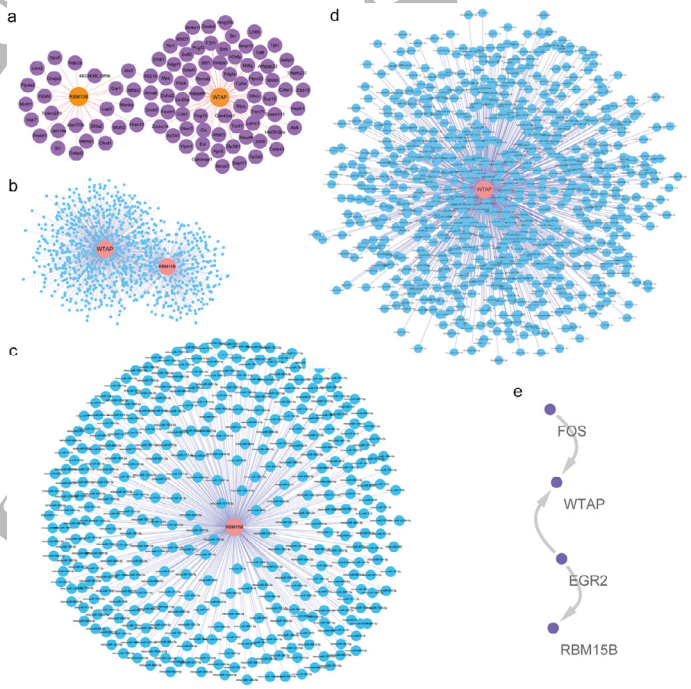

Figure 8: PPI network of the Hub m6A regulator: a. Hub m6A regulatory factor PPI network, b-d. Hub m6A regulatory factor miRNA network, e. Hub m6A regulatory factor TFs network.

To further observe the effect of hub m6A regulators on brain tissue in ASD samples, we performed a single-gene GSEA (ssGSEA) for both genes (Figure 8). The GO attributes of gene RBM15B were notably enriched in processes, such as neutral amino acid transport, positive regulation of epidermal cell differentiation, enhancement of epidermal development, promotion of focal adhesion assembly, regulation of the endocytic cycle, responses to platelet-derived growth factor, glycoprotein complex, 2a protein phosphatase complex, pyrimidine bundle binding, RNA cap binding, and other functions. The enriched KEGG pathways included lipid metabolism (fatty acids and linoleic acid), amino acid breakdown (lysine and tryptophan), central metabolism (glyoxylate cycle and pentose phosphate), signaling (MAPK and VEGF), and *Vibrio cholerae* infection processes. GO enrichment included apical protein localization, endocytic recycling, neutral amino acid transport, positive regulation of epidermal cell differentiation, positive regulation of epidermal development, positive regulation of focal adhesion assembly, regulation of endocytic recycling, protein phosphatase type 2a complex, and polypyrimidine tract binding. KEGG pathways were enriched in alpha-linolenic acid metabolism, cysteine and methionine metabolism, fatty acid metabolism, homologous recombination, lysosomes, the MAPK signaling pathway, glycan biosynthesis, oocyte meiosis, the pentose phosphate pathway, and the VEGF signaling pathway(Figure 9).

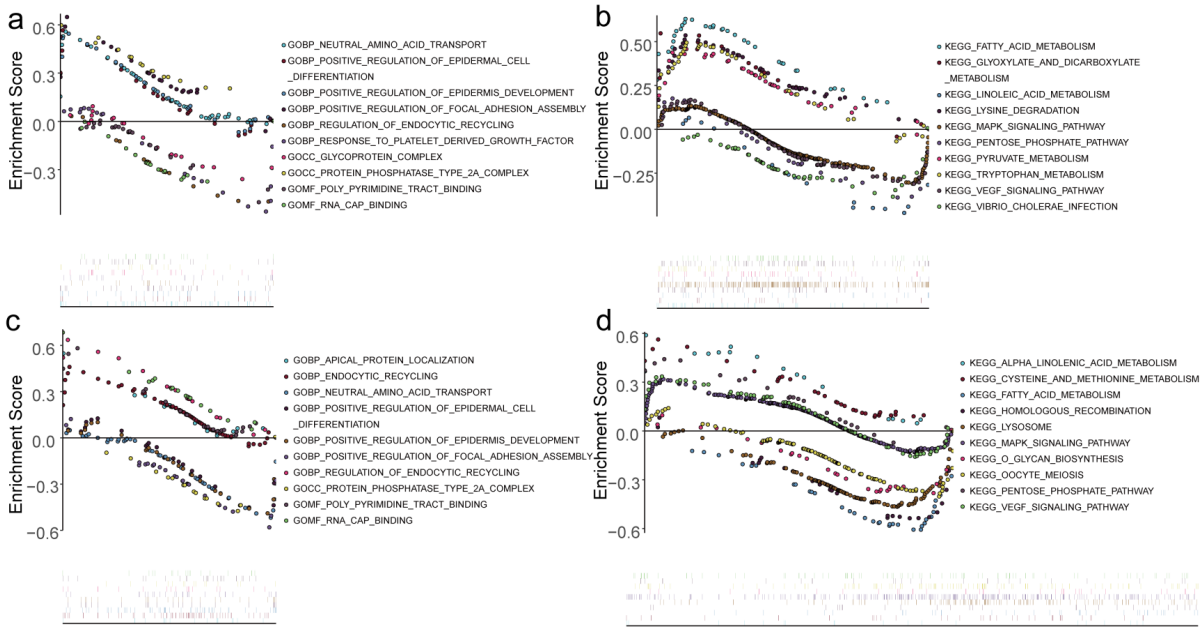

Figure 9: Single-gene GSEA enrichment analysis of the Hub m6A regulator: a. GSEA-GO analysis of RBM15B, b. GSEA-KEGG analysis of RBM15B, c. GSEA-GO analysis of WTAP, d. GSEA-KEGG analysis of WTAP.

2.8. Immune Cell Infiltration Analysis in ASD Samples

To evaluate the characteristics of immune cell infiltration within the brain tissue of ASD samples and explore the potential associations between key immune cell infiltration and immunotherapy efficacy, we calculated the infiltration levels of 29 distinct immune cell types in each tissue sample using ssGSEA. Co-expression analyses revealed that immune components, such as parainflammation-associated cells, activated dendritic cells (aDCs), neutrophils, tumor-infiltrating lymphocytes (TIL), T-cell co-stimulation, T-cell co-inhibition, checkpoint cells, and regulatory T cells (Tregs) exhibited strong correlations with the majority of immune cells (Figure 10a). Subsequently, we performed a correlation analysis between essential m6A regulatory factors and the immune microenvironment. By examining the relationship between ssGSEA outcomes and key genes, we found that gene RBM15B demonstrated a significant positive correlation with the number of dendritic cells, antigen-presenting cells (APCs), co-inhibitory T cells, Tregs, and inflammation. Conversely, gene RBM15B negatively correlated with the levels of costimulatory T cells, T helper cells, immune checkpoints, and Type II interferon responses. Gene WTAP displayed marked correlations with dendritic cells, APCs, B cells, immune checkpoint molecules, Tregs, and costimulatory T cells. However, gene WTAP was negatively correlated with neutrophils, parainflammation, co-inhibitory T cells, and TILs (Figure 10b–d, Figure 11).

To further investigate the biological characteristics of various tissues in ASD samples from an immunological perspective, we used the expression profiles of 29 immune cell gene sets to conduct hierarchical clustering of ASD samples, successfully categorizing all samples into two distinct groups (Group I: n = 4; Group II: n = 4; Figure 10e-g). Subsequent differential analysis of hub m6A modifiers in Groups I and II revealed notable disparities in WTAP and RBM15B expression levels across different immune cohorts ($P < 0.05$) (Figure 10h–i).

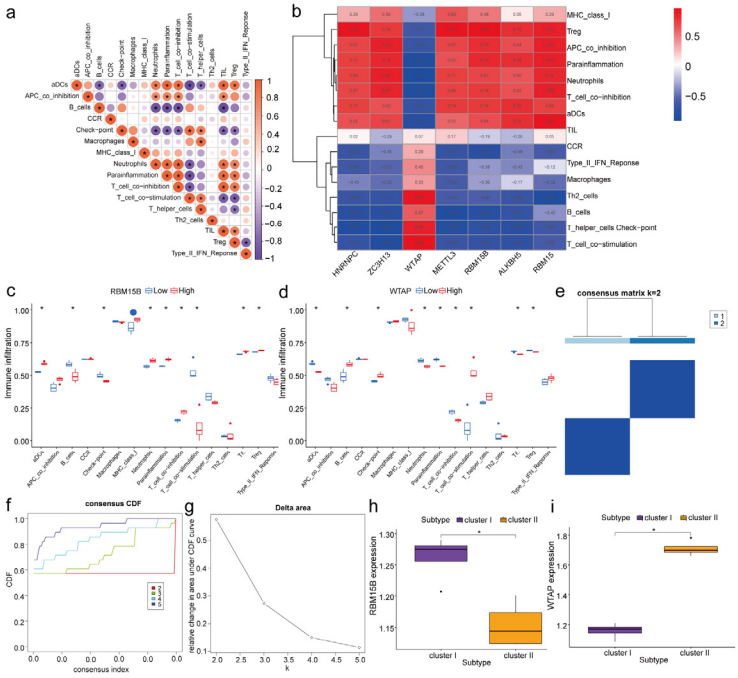

Figure 10: Molecular isoform construction of differential genes in ASD: a. Immunocyte co expression analysis; b. Correlation analysis between differentially expressed m6A regulatory factors and immune cells; c: Correlation analysis between RBM15B gene expression and immune cells; d. Correlation analysis between WTAP gene expression and immune cells; e-g: Sample clustering grouping based on immune cell content, e: Sample size after grouping; f: The area under CDF and its relative variation with increasing k; g: The Delta area plot displays the relative change in area under the CDF curve; h: Validation of RBM15B expression in different immune subtypes; i. Validation of WTAP expression in different immune subtypes, with purple representing Cluster I and orange representing Cluster II.

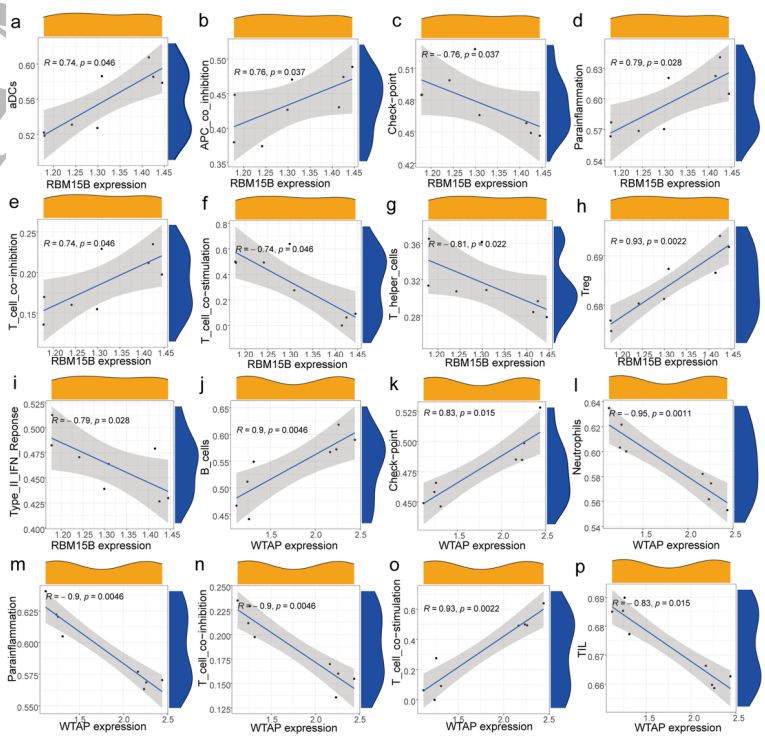

Figure 11: Correlation analysis of m6A regulators with immune cell infiltration: a-i. Correlation analysis between immune cells and RBM15B, Correlation analysis between j-p. immune cells and WTAP.

2.9. Immune Cell Infiltration in ASD

To delineate the immune microenvironment composition in ASD,we applied the ssGSEA algorithm to quantify the infiltration levels of 29 distinct immune cell types in both ASD and normal tissues. The Wilcoxon test indicated that six immune cell types exhibited significant overexpression in normal tissues (Figure 12b–d), namely aDCs, neutrophils, parainflammation, T-cell co-inhibition, TIL, and Tregs. In addition, three immune cells were significantly overexpressed in the brain tissue of ASD samples.

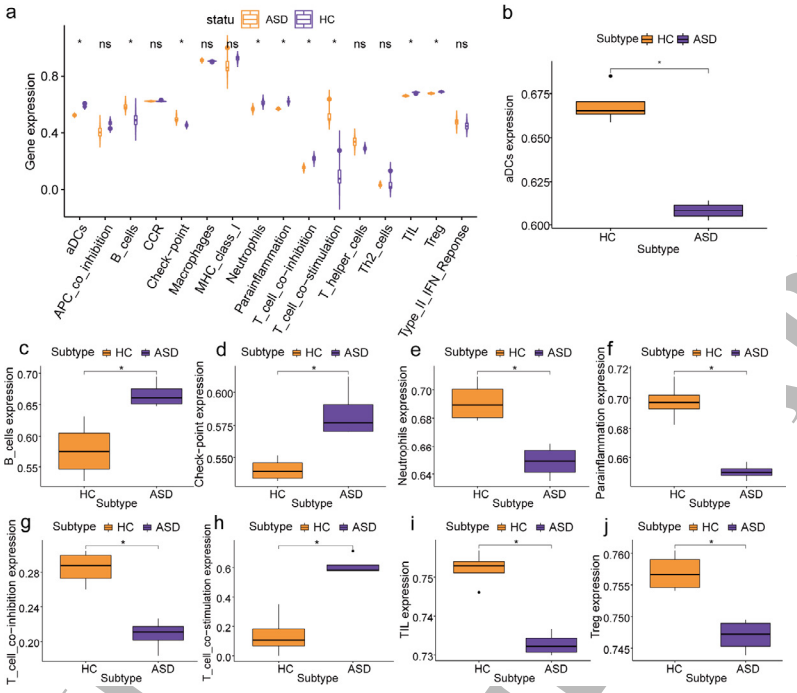

Figure 12: Differential analysis of immune infiltration: a. Differential analysis of immune cell infiltration levels between ASD and normal groups, b-j: Box plot analysis of differences in infiltration of different immune cells.

2.10. Molecular ASD Subtypes and related Analysis

Unsupervised clustering of differentially expressed genes in ASD revealed functional networks of hub m6A regulators. This analysis resulted in the classification of all samples into two distinct isoforms (Isoform A n = 4; Isoform B: n = 4; Figure 13a–c). The results of the (PCA demonstrated a considerable degree of separation (Figure 13d), and the subsequent differential analysis of key m6A regulators in groups A and B indicated significant differences in WTAP and RBM15B expression across these groups ($P < 0.05$, Figure 14).

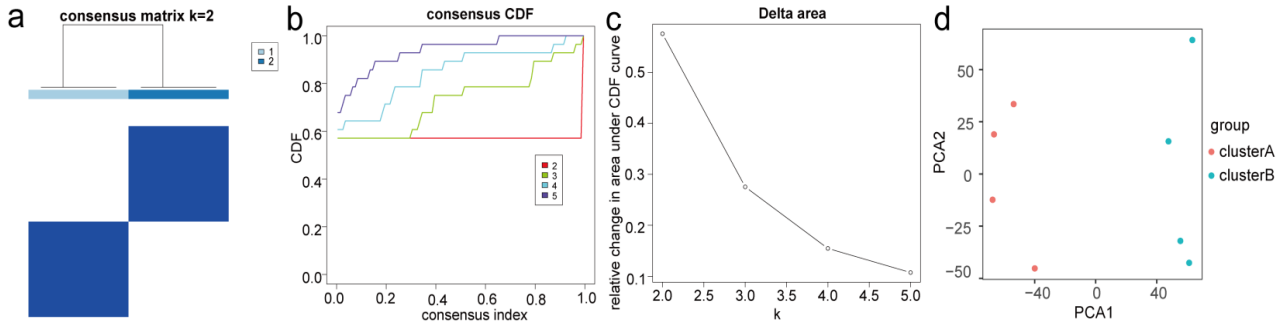

Figure 13: Construction of ASD molecular subtypes: a-c□Cluster grouping of ASD samples based on significantly differentially expressed gene expression, a: Sample size after grouping; b: The area under CDF and its relative variation with increasing k; c: The Delta area plot displays the relative change in area under the CDF curve; d: PCA analysis under Cluster A and Cluster B grouping, where red represents Cluster A and blue represents Cluster B.

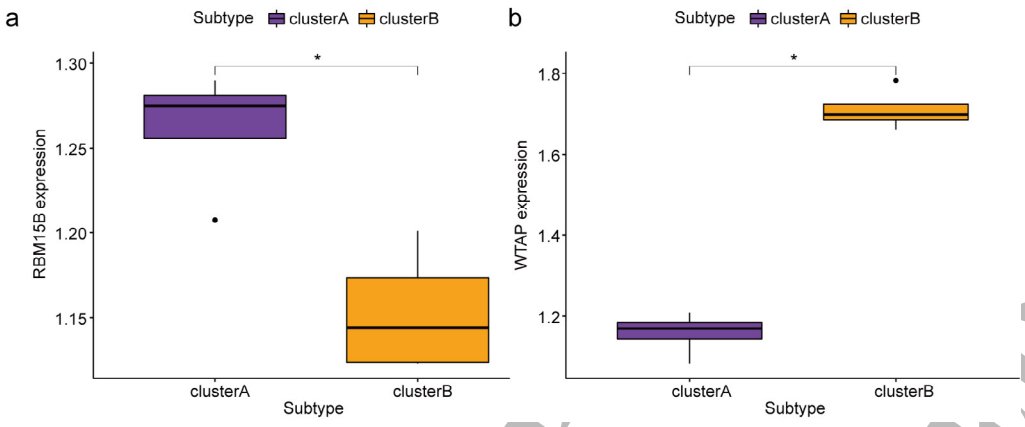

Figure 14: Correlation analysis between hub m6A and molecular subtypes of ASD: a. RBM15B differential expression analysis, b. WTAP differential expression analysis, purple represents Cluster A, orange represents Cluster B

3. Discussion

The prevalence of ASD is increasing annually and garnering increasing attention. Currently, limited effective treatment methods are available, highlighting the urgent need for extensive exploration into the pathogenesis of ASD to identify effective intervention approaches.

Our study findings align with previous research that demonstrated significant gene expression changes in ASD. For example, Wang *et al*. identified altered m6A profiles in cardiac tissues, showing that differential gene expression is closely associated with m6A modifications, which might also be relevant in ASD [7]. Furthermore, functional enrichment analysis indicated that ASD brain tissues are predominantly enriched in aerobic respiration and amide biosynthetic processes. These findings are consistent with the notion that ASD may share common pathological mechanisms with other neurological disorders [8].

Our GSVA revealed 49 significantly upregulated and 53 downregulated GO functions in ASD tissues, contributing to an understanding of autistic-associated biological characteristics. This is supported by studies on other diseases, such as osteoarthritis, where m6A modification and immune microenvironment infiltration patterns differ significantly between healthy and diseased tissues [9]. M6A regulatory factors exhibited significant differential expression in ASD samples, which is consistent with the results of other investigations, including those concentrating on systemic lupus erythematosus (SLE), where m6A epitranscriptome serves as molecular rheostats coordinating mRNA metabolism and innate immunity activation via pattern recognition receptors, similar to their roles in other diseases, such as myocardial injury and renal cell carcinoma [10-12]. Immune infiltration analysis revealed that aDCs and neutrophils were highly expressed in normal tissues, whereas B cells and checkpoint molecules were elevated in ASD tissues. This suggests the presence of a distinct immune microenvironment in ASD, which is supported by studies showing that m6A modifications regulate immune responses during bacterial and viral infections [13].

Several statistical models were comprehensively and complementarily used to explore the relationships between specific exposures and outcomes. These findings were supported by GSEA, which revealed that ASD brain tissues were predominantly enriched in GO functions such as aerobic respiration and amide biosynthetic processes, as well as KEGG analysis revealed pathways mediating polyglutamine disorders (Huntington's) and amyloid pathologies (Alzheimer's). These results highlight the potential involvement of similar pathological mechanisms in ASD.

Furthermore, GSVA provided a detailed view of functional changes, identifying 49 significantly upregulated and 53 significantly downregulated GO functions in ASD tissues. This method offers a complementary perspective by highlighting the specific biological processes altered in ASD, thereby enhancing our understanding of the biological characteristics of the disease. In the context of m6A regulatory factors, LASSO regression was used alongside SVM-RFE algorithms to identify pivotal m6A regulators. The LASSO model identified WTAP, METTL3, RBM15B, ALKBH5, and RBM15 as critical m6A regulators, whereas the SVM-RFE algorithm identified WTAP and RBM15 as key feature genes. These methods aimed to identify the most relevant m6A regulators associated with ASD, with both approaches yielding consistent results that reinforce the importance of these factors in the pathology of the disease.

Additionally, Immunological profiling demonstrated notable differences in immune cell populations between ASD and normal tissues. Specifically, aDCs and neutrophils were highly expressed in normal tissues, whereas B and checkpoint cells were more prevalent in ASD tissues than in normal tissues. In the early defense stage, neutrophils regulate inflammatory responses through phagocytosis, enzyme release, and the release of chemical substances. B-cells are responsible for humoral immunity and produce antibodies that specifically target and eliminate pathogens. aDC and checkpoint cells activate T cells, thereby maintaining the immune balance in the body. This analysis aimed to elucidate the role of the

immune microenvironment in ASD, with the findings suggesting a distinct immune landscape that might influence disease progression and therapeutic responses.

The use of multiple models from different dimensions collectively revealed a consistent and robust relationship between specific exposures and outcomes in ASD. Each model's findings reinforced the others, providing a comprehensive and convincing conclusion regarding the molecular and immunological underpinnings of ASD. This multifaceted approach enhanced the credibility of the study by demonstrating the consistency and reproducibility of the results across diverse analytical approaches.

The differential expression of m6A regulatory genes in patients with ASD, as identified in our investigation, underscores the significant role of m6A methylation in ASD pathophysiology. M6A methylation is a crucial post-transcriptional modification that affects mRNA stability, splicing, and translation, thereby influencing gene expression and protein production [14]. The observed differential expression of m6A regulatory genes, such as RBM15, ZC3H13, METTL3, HNRNPC, RBM15B, ALKBH5, and WTAP, suggests that alterations in m6A methylation patterns could contribute to the molecular mechanisms underlying ASD. Our findings align with those of previous studies indicating the involvement of m6A methylation in neuropsychiatric disorders, including Liufu et al. (2024) demonstrated that m6A methylation is implicated in various neuropsychiatric diseases by regulating gene expression and protein production [15]. This study supports the notion that the m6A modification influences ASD development and progression via similar mechanisms.

The identification of key m6A regulatory factors, such as METTL3 and RBM15B, using LASSO and SVM-RFE algorithms further highlights their potential as critical modulators in ASD. METTL3, in particular, reduces hippocampal neuron apoptosis in an autism mouse model by modulating the MALAT1/SFRP2/Wnt/β-catenin pathway, suggesting a neuroprotective role [16]. This finding is consistent with our results, which indicate that METTL3 is differentially expressed in patients with ASD and potentially contributes to altered neuronal function and survival. Moreover, the significant correlation between hub m6A regulatory factors and immune cell infiltration levels in ASD samples suggests that m6A methylation may influence the immune microenvironment in ASD samples. This finding is supported by the evidence that m6A modifications regulate immune responses and inflammation, which are implicated in the pathogenesis of ASD [17]. The differential infiltration of immune cell types, such as aDCs, neutrophils, B cells, and checkpoint cells, between ASD and normal tissues further emphasizes the significance of immune dysregulation in ASD.

Considering the limitations of this study, the following points warrant attention. First, the analysis was conducted solely using bioinformatics approaches without the integration of laboratory experiments, which could provide additional validation and mechanistic insights into the findings. Second, the sample size used in the GEO database was comparatively small, possibly restricting the generalizability of the results. Furthermore, the absence of clinical validation is a critical gap, as it is necessary to confirm the relevance of the identified m6A regulatory factors in patients with ASD. Additionally, using multiple datasets could introduce batch effects, which might affect the consistency and reliability of the differential expression analysis.

In conclusion, our study provides strong evidence that m6A methylation is pivotal for ASD by modulating gene expression, neuronal function, and immune responses. The differential expression of m6A regulatory genes and their correlation with immune cell infiltration levels highlight the intricate interaction between epigenetic modifications and the immune system in ASD. Subsequent research needs to focus on clarifying the specific molecular mechanisms through which m6A methylation affects ASD pathophysiology and explore potential therapeutic targets within this pathway. Subsequent investigations incorporating extensive sample quantities, clinical validation, and experimental approaches are vital to fully elucidate the implications of m6A modifications in ASD and translate these findings into clinical applications.

4. Methods

4.1. Transcriptomic data Acquisition and DEG Analysis

Gene expression datasets comprising clinical specimens ASD were collected from the GSE156646 accession of the National Center for Biotechnology Information (NCBI) GEO repository (https://www.ncbi.nlm.nih.gov/geo/query/acc.cgi?acc=GSE156646) [18,19]. This dataset consists of eight samples, including four ASD samples and four normal controls. The gene set comprising m6A (N6-Methyladenosine) modified genes was sourced from the work of Wang et al., encompassing seven RBM15 writers, namely ZC3H13, METTL3, WTAP, CBLL1, METTL16, and RBM15B [20]. The m6A-binding proteome comprised two functionally distinct subgroups: cytoplasmic readers (YTHDF1/2/3) and nuclear regulators (YTHDC1, HNRNPA2B1, and HNRNPC). There were two errors in total: ALKBH5 and FTO. To investigate the expression dynamics of m6A-related modulators within cerebral tissues from ASD murine models, we conducted differential expression analysis between samples from patients with ASD and normal controls using the Limma package in R [21]. Gene expression changes were classified as significant if meeting $|logFC| \geq 1$ (FDR < 0.05), with upregulated ($logFC > 1$) and downregulated ($logFC < -1$) clusters analyzed separately.

4.2. Functional Enrichment Analysis and Co-Expression Analysis

GSEA was utilized to assess the distribution patterns of genes within predefined gene sets, organized by their correlation with specific phenotypes, and ascertain their contribution to the phenotype [22]. We acquired the gene sets labeled "c2.egg.v7.4. symbols" and "c5.go.v7.4. symbols" from the MSigDB database (http://www.gsea-msigdb.org/gsea/index.jsp) and performed GSEA for both gene sets within the ASD and normal control cohorts [23]. The "clusterProfiler" R package was used for GSEA, and $P < 0.05$ was regarded as statistically significant [24,14]. GSVA, a nonparametric and unsupervised analytical technique, was used to evaluate the

enrichment results of gene sets within the chip nuclear transcriptome. This method assesses whether distinct metabolic pathways are enriched across various samples by transforming the expression level matrix of genes into a matrix reflecting the gene set expression levels between the samples. We executed GSVA on the gene sets "c2.egg.v7.4. symbols" and "c5.go.v7.4. symbols" for both ASD and normal control groups, used the "GSVA" R package to the enrichment analysis, and visualized them using the "pheatmap" package [25].

To explore the modifications in the expression of m6A regulatory elements within ASD brain tissue, we extracted data pertaining to 23 m6A regulatory factors from the ASD dataset. Subsequently, we used the Limma package version 4 within R to recognize and filter differentially expressed modified genes by comparing ASD samples to normal samples and performed co-expression analysis on these modified genes. Finally, we examined the chromosomal localization of the modified genes.

4.3. m6A Methylation Modification Factor Molecular Subtype Construction

We used differential expression of m6A regulatory factors and performed cluster analysis on the samples using the "ConsensusClusterPlus" package in R language [26]. The samples were categorized into distinct groups based on the differential expression of the m6A regulatory factors observed in each sample, with parameters configured for 50 repetitions (reps = 50) and a resampling rate of 80% (pItem = 0.8). To validate the grouping, we conducted PCA on the expression profiles of all genes and used the "ggplot2" package to visualize the results.

4.4. Hub m6A Regulatory Factor Screening

A predictive model was constructed using ASD differentially expressed RNA-modified genes. A LASSO regression analysis was performed on the training dataset using the R glmnet package [27]. The LASSO algorithm facilitates dimensionality reduction in high-dimensional datasets using a model characterized by a reduced number of variables to elucidate data features. To mitigate the risk of overfitting the model derived from the training dataset, we implemented a ten-fold cross-validation approach. Finally, a stratification model was formulated by applying the regression coefficients generated through LASSO regression analysis. Subsequently, we further screened genes using a support vector machine (SVM) algorithm and analyzed the differentially expressed m6A regulatory factors between the normal and ASD groups. We used the Support Vector Machine Recursive Feature Elimination (SVM-RFE) machine learning algorithm. The LASSO model intersects feature genes to isolate key genes.

4.5. Hub Regulatory Factor Interaction Network Construction

The protein interaction network comprises individual proteins that engage in various biological processes such as signal transduction, regulation of gene expression, metabolism of energy and substances, and modulation of the cell cycle through their interactions. A comprehensive analysis of the interactions among numerous proteins within biological systems is crucial for elucidating the operational principles of proteins, understanding the mechanisms of biological signal responses and energy metabolism under specific physiological conditions, such as diseases, and discerning the functional interconnections among proteins. We used StarBase2.0 (http://starbase.sysu.edu.cn/) to systematically identify RNA-RNA and protein-RNA interaction networks, leveraging this database to uncover the regulatory relationships of hub m6A regulatory factor proteins and visualized these relationships using Cytoscape software (version: 3.9.0).

MiRNA- or TF-controlled gene expression has been analyzed at the post-transcriptional stage by limiting disease conditions through interactions with target genes [28,29]. We obtained miRNAs in the miRWalk database (http://mirwalk.umm.uni-heidelberg.de) related to hub m6A regulatory factors in ASD. MiRWalk is a comprehensive open-source miRNA target gene database platform that includes miRNA target gene information from multiple species such as humans, mice, rats, dogs, and cows. MiRWalk also integrates information from databases, such as miRDB, TargetScan, and miRTarBase [30]. Transcription factors were obtained from HumanTF (The Human Transcription Factors) (http://humantfs.ccbr.utoronto.ca). Subsequently, Spearman correlation analysis was conducted on TFs and hub m6A regulatory factors, with screening criteria of cor > 0.4 and P < 0.01. Additionally, we visualized the miRNA network linked to X-related hub m6A regulatory factors and the transcription factor (TFs) network related to these hub m6A regulatory factors using Cytoscape software(version:3.9.0).

4.6. Single-Gene GSEA Enrichment Analysis

GSEA 4.0.3 software was used to perform GSEA detection on hub m6A regulatory factors. The cohort was dichotomized using median-split stratification based on the transcriptional abundance profiles of hub m6A epitranscriptomic modulators. Specifically, the samples were classified into high- (exceeding median expression) and low-expression cohorts (below median). The gene set database used for this analysis was c2.kg.v7.4. symbols.gmt and c5.go.v7.4. symbols.gmt. Each analysis included 1000 genome permutations.

4.7. Immune Infiltration Analysis

ssGSEA extends on the traditional GSEA by enabling pathway-level enrichment scoring for individual samples. This principle is similar to that of the GSEA [31]. In a study conducted by Yin et al., we extracted 29 immune-related gene sets and assessed the degree of immune contexture in each sample based on the expression levels of specific marker genes associated with immune cells. ssGSEA was implemented using the "GSVA" package in R. Immune infiltration analysis was performed on both the ASD and normal groups using the Limma package, which allowed us to identify immune cells that exhibited differential enrichment between the ASD and control groups across the two datasets. The association between immune infiltration levels and the expression profiles of pivotal genes was assessed using Pearson's correlation analysis.

4.8. Immune Infiltration-Related Molecular Subtype Construction

Based on the ssGSEA algorithm, we used "ConsensusClusterPlus" 10 in R language(http://www.bioconductor.org/packages/release/bioc/html/ConsensusClusterPlus.html). Cluster analysis was performed, and the samples were systematically categorized into various groups based on the expression profiles of m6A regulatory factors within each sample. Parameters were established to repeat the analysis 50 times (reps = 50), with the resampling rate set at 80% (pItem = 0.8). To assess the robustness of the grouping, PCA was conducted on the expression levels of all genes, with the results visualized using the "ggplot2" package.

4.9. Molecular Subtypes of Key Genes in ASD

We used significantly different genes (logFC >1.5, $P < 0.05$) between ASD and control group tissues, and "ConsensusClusterPlus" 10 in R (http://www.bioconductor.org/packages/release/bioc/html/ConsensusClusterPlus.html). We performed unsupervised clustering of the samples using the expression profiles of autistic-associated DEGs and revealed distinct subgroups. Parameters were configured to execute 50 repetitions (reps = 50) at a resampling rate of 80% (pItem = 0.8). To assess the validity of the classifications, PCA was conducted on the expression levels of all genes, and the outcomes were visualized using the "ggplot2" package. Finally, a correlation test was conducted between the ASD key genes and molecular subtypes.

4.10. Statistical Analysis

R (https://www.r-project.Org) was used to conduct statistical assessments and data computations. For the comparison of two consecutive variables, the statistical significance of normally distributed variables was estimated using an independent Student's t-test, and the differences between non-normally distributed variables were analyzed using the Mann–Whitney U test (Wilcoxon rank-sum test). $P < 0.05$ (two-tailed tests) was considered significant.

Acknowledgments

Thank for the support provided by Xiantao Academic.

Author Contributions

Li Yao: Methodology, Formal analysis, and Writing - Original Draft. Yihuan Yue: Writing the original draft, writing the review, and editing. Jinhui Wang: Funding acquisition, Supervision, Project administration.

Funding

Open access funding provided by Natural Science Foundation of Fujian Province 2021D030.

Data Availability Statement

Gene expression data from the GEO repository (https://www.ncbi.nlm.nih.gov/geo/) include the following datasets: GSE156646. The m6A (N6-Methyladenosine) modified gene set was sourced from Wang Y et al.

Additional Information

Ethics Approval and Consent to Participate: Not applicable.

Competing Interests: The authors declare no conflicts of interest pertaining to this work.

References

1. Zeidan, J., Fombonne, E., Scorah, J., Ibrahim, A., Durkin, M. S., Saxena, S., ... & Elsabbagh, M. (2022). Global prevalence of autism: A systematic review update. *Autism research, 15*(5), 778-790.
2. Tsao, C. Y., & Mendell, J. R. (2007). Autistic disorder in 2 children with mitochondrial disorders. *Journal of child neurology, 22*(9), 1121-1123.
3. Spiroski, M., Trajkovski, V., Trajkov, D., Petlichkovski, A., Efinska-Mladenovska, O., Hristomanova, S., ... & Bozhikov, J. (2009). Family analysis of immunoglobulin classes and subclasses in children with autistic disorder. *Bosnian journal of basic medical sciences, 9*(4), 283.
4. Dhossche, D., Applegate, H., Abraham, A., Maertens, P., Bland, L., Bencsath, A., & Martinez, J. (2002). Elevated plasma gamma-aminobutyric acid (GABA) levels in autistic youngsters: stimulus for a GABA hypothesis of autism. *Medical science monitor: international medical journal of experimental and clinical research, 8*(8), PR1-6.
5. Bradley, S., Moore, F., Duffy, F., Clark, L., Suratwala, T., Knightsmith, P., & Gillespie-Smith, K. (2024). Camouflaging, not sensory processing or autistic identity, predicts eating disorder symptoms in autistic adults. *Autism, 28*(11), 2858-2868.
6. Schröder, S. S., Danner, U. N., Spek, A. A., & van Elburg, A. A. (2023). Exploring the intersection of autism spectrum disorder and eating disorders: understanding the unique challenges and treatment considerations for autistic women with eating disorders. *Current opinion in psychiatry, 36*(6), 419-426.
7. Wang, W., Zhang, T. N., Yang, N., Wen, R., Wang, Y. J., Zhang, B. L., ... & Liu, C. F. (2023). Transcriptome-wide identification of altered RNA m6A profiles in cardiac tissue of rats with LPS-induced myocardial injury. *Frontiers in Immunology, 14*, 1122317.
8. Gao, S., Wang, Y., Li, X., Liang, Y., Jin, Z., Yang, B., ... & Rao, Y. (2024). Dynamics of N6-methyladenosine modification during Alzheimer's disease development. *Heliyon, 10*(6).
9. Ouyang, Y., Tu, Y., Chen, S., Min, H., Wen, Z., Zheng, G., ... & Sun, G. (2022). Characterization of immune microenvironment infiltration and m6A regulator-mediated RNA methylation modification patterns in osteoarthritis. *Frontiers in Immunology, 13*, 1018701.
10. Li, L. J., Fan, Y. G., Leng, R. X., Pan, H. F., & Ye, D. Q. (2018). Potential link between m6A modification and systemic lupus erythematosus. *Molecular immunology, 93*, 55-63.
11. Zhang, X., Zhang, S., Yan, X., Shan, Y., Liu, L., Zhou, J., ... & Lai, W. (2021). m6A regulator-mediated RNA methylation modification patterns are involved in immune microenvironment regulation of periodontitis. *Journal of Cellular and Molecular Medicine, 25*(7), 3634-3645.

12. Gan, Y., Li, A., Liu, J., Wang, X., Zhang, Z., Li, Q., ... & Zhang, Q. (2022). m6A-mRNA methylation regulates gene expression and programmable m6A modification of cellular RNAs With CRISPR-Cas13b in renal cell carcinoma. *Frontiers in Genetics, 12*, 795611.
13. Feng, J., Zhang, T., Sorel, O., Meng, W., Zhang, X., Lai, Z., ... & Gao, S. J. (2022). Global profiling reveals common and distinct N6-methyladenosine (m6A) regulation of innate immune responses during bacterial and viral infections. *Cell Death & Disease, 13*(3), 234.
14. Sanderson, M. R., Fahlman, R. P., & Wevrick, R. (2021). The N-terminal domain of the Schaaf–Yang syndrome protein MAGEL2 likely has a role in RNA metabolism. *Journal of Biological Chemistry, 297*(2).
15. Liufu, C., Luo, L., Pang, T., Zheng, H., Yang, L., Lu, L., & Chang, S. (2024). Integration of multi-omics summary data reveals the role of N6-methyladenosine in neuropsychiatric disorders. *Molecular psychiatry, 29*(10), 3141-3150.
16. Ming, Y., Deng, Z., Tian, X., Jia, Y., Ning, M., & Cheng, S. (2022). m6A methyltransferase METTL3 reduces hippocampal neuron apoptosis in a mouse model of autism through the MALAT1/SFRP2/Wnt/β-catenin axis. *Psychiatry Investigation, 19*(10), 771.
17. Zhang, C., Fu, J., & Zhou, Y. (2019). A review in research progress concerning m6A methylation and immunoregulation. *Frontiers in immunology, 10*, 922.
18. Mizuno, S., Hirota, J. N., Ishii, C., Iwasaki, H., Sano, Y., & Furuichi, T. (2020). Comprehensive profiling of gene expression in the cerebral cortex and striatum of BTBRTF/ArtRbrc mice compared to C57BL/6J mice. *Frontiers in cellular neuroscience, 14*, 595607.
19. Barrett, T., Troup, D. B., Wilhite, S. E., Ledoux, P., Rudnev, D., Evangelista, C., ... & Edgar, R. (2007). NCBI GEO: mining tens of millions of expression profiles—database and tools update. *Nucleic acids research, 35*(suppl_1), D760-D765.
20. Wang, Y., Li, L., Li, J., Zhao, B., Huang, G., Li, X., ... & Zhou, Z. (2021). The emerging role of m6A modification in regulating the immune system and autoimmune diseases. *Frontiers in Cell and Developmental Biology, 9*, 755691.
21. Ritchie, M. E., Phipson, B., Wu, D. I., Hu, Y., Law, C. W., Shi, W., & Smyth, G. K. (2015). limma powers differential expression analyses for RNA-sequencing and microarray studies. *Nucleic acids research, 43*(7), e47-e47.
22. Subramanian, A., Tamayo, P., Mootha, V. K., Mukherjee, S., Ebert, B. L., Gillette, M. A., ... & Mesirov, J. P. (2005). Gene set enrichment analysis: a knowledge-based approach for interpreting genome-wide expression profiles. *Proceedings of the National Academy of Sciences, 102*(43), 15545-15550.
23. Liberzon, A., Birger, C., Thorvaldsdóttir, H., Ghandi, M., Mesirov, J. P., & Tamayo, P. (2015). The molecular signatures database hallmark gene set collection. *Cell systems, 1*(6), 417-425.
24. Yu, G., Wang, L. G., Han, Y., & He, Q. Y. (2012). clusterProfiler: an R package for comparing biological themes among gene clusters. *Omics: a journal of integrative biology, 16*(5), 284-287.
25. Hänzelmann, S., Castelo, R., & Guinney, J. (2013). GSVA: gene set variation analysis for microarray and RNA-seq data. *BMC bioinformatics, 14*, 1-15.
26. Wilkerson, M. D., & Hayes, D. N. (2010). ConsensusClusterPlus: a class discovery tool with confidence assessments and item tracking. *Bioinformatics, 26*(12), 1572-1573.
27. Friedman, J. H., Hastie, T., & Tibshirani, R. (2010). Regularization paths for generalized linear models via coordinate descent. *Journal of statistical software, 33*, 1-22.
28. Soifer, H. S., Rossi, J. J., & Sætrom, P. (2007). MicroRNAs in disease and potential therapeutic applications. *Molecular therapy, 15*(12), 2070-2079.
29. Baldwin, A. S. (2001). Series introduction: the transcription factor NF-κB and human disease. *The Journal of clinical investigation, 107*(1), 3-6.
30. Sticht, C., De La Torre, C., Parveen, A., & Gretz, N. (2018). miRWalk: an online resource for prediction of microRNA binding sites. *PloS one, 13*(10), e0206239.
31. Guo, C., Liu, Z., Cao, C., Zheng, Y., Lu, T., Yu, Y., ... & Li, Z. (2022). Development and validation of ischemic events related signature after carotid endarterectomy. *Frontiers in Cell and Developmental Biology, 10*, 794608.